

**Electroproduction of forward protons up to  $Q^2 = 9.5 \text{ GeV}^{2*}$**

C. J. Bebek, C. N. Brown,<sup>†</sup> R. V. Kline, F. M. Pipkin, S. W. Raither, and L. K. Sistrerson<sup>‡</sup>  
*High Energy Physics Laboratory, Harvard University, Cambridge, Massachusetts 02138*

A. Browman,<sup>§</sup> K. M. Hanson,<sup>§</sup> D. Larson, and A. Silverman  
*Laboratory of Nuclear Studies, Cornell University, Ithaca, New York 14853*

(Received 28 October 1976)

We report new measurements of inclusive proton electroproduction. Data were taken with a hydrogen target at the  $(W, Q^2)$  points  $(2.2 \text{ GeV}, 1.2 \text{ GeV}^2)$ ,  $(2.7, 2.0)$ ,  $(2.7, 3.3)$ ,  $(2.7, 6.2)$ , and  $(2.7, 9.5)$  and with a deuterium target at  $(2.2, 1.2)$ ,  $(2.7, 2.0)$ ,  $(2.7, 6.2)$ , and  $(2.7, 9.5)$ . The invariant structure function is studied as a function of  $W$ ,  $Q^2$ ,  $\omega$ , and  $x'$ . The data are compared with the predictions of the constituent-interchange model.

I. INTRODUCTION

The extension of the quark-parton model to the inclusive electroproduction cross sections predicts that the invariant cross sections normalized by the total virtual-photon-production cross section will exhibit Bjorken scaling when expressed as a function of the Feynman variables  $x'$  and  $p_T^2$ .<sup>1</sup> This prediction has been verified for inclusive pion electroproduction in the forward direction<sup>2</sup> and shown to be approximately true for pions and protons produced near  $90^\circ$  in the virtual-photon-target-proton center-of-mass system.<sup>3,4</sup> Both the pions and protons produced near  $90^\circ$  show a scaling behavior suggestive of the constituent-interchange model. Earlier reported measurements showed that the inclusive cross section for forward protons does not show Bjorken scaling.<sup>5,6</sup> This paper extends these tests of the parton model to forward protons produced at higher  $Q^2$  for both hydrogen and deuterium targets and compares the scaling behavior with that observed for protons produced at large angles.

II. KINEMATICS

Measurements of the inclusive proton electroproduction reaction

$$e + N \rightarrow e + p + \text{anything} \tag{1}$$

were carried out at the Wilson Synchrotron Laboratory at Cornell University. Reaction (1) is analyzed in terms of the virtual-photon-production reaction

$$\gamma_\nu + N \rightarrow p + \text{anything}, \tag{2}$$

where the virtual-photon mass squared,  $-Q^2$ , energy,  $\nu$ , direction, and polarization parameter,  $\epsilon$ , are tagged by the scattered electron. The cross section for reaction (1) is written<sup>7</sup>

$$\frac{d\sigma}{d\Omega_e dE' dp^3} = \Gamma \frac{d^3\sigma}{dp^3}, \tag{3}$$

where  $\Gamma$  is the "flux" of virtual photons and  $d^3\sigma/dp^3$  is the cross section for reaction (2). The virtual-photon-production cross section is a function of  $W$  (the virtual-photon-nucleon center-of-mass energy),  $Q^2$ ,  $\epsilon$ ,  $p_T$  (the component of the proton momentum normal to the direction of the virtual photon),  $x' = p_{\parallel}^*/(p_{\text{max}}^* - p_T^2)^{1/2}$  (the component of the proton momentum parallel to the direction of the virtual photon normalized to the maximum longitudinal momentum consistent with the value of  $p_T$ ), and  $\phi$  (the angle between the electron-virtual-photon plane and the virtual-photon-proton plane). The asterisk denotes the virtual-photon-target-nucleon center of mass and  $p_{\text{max}}^*$  is the maximum proton momentum kinematically allowed using the  $p\pi^0$  final state. The virtual-photon-production cross section is a function of  $\phi$  of the form

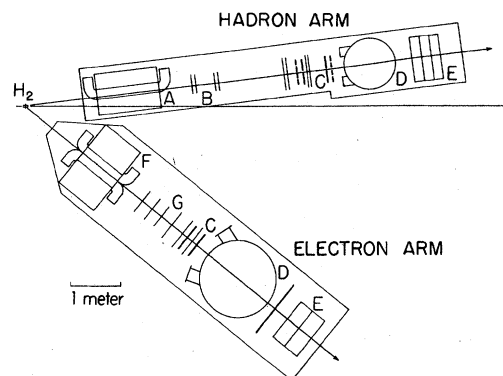


FIG. 1. A schematic view of the apparatus. A and F: bending magnets, B: multiwire proportional counters, C: scintillation counters, D: Freon Čerenkov counters, E: lead-Lucite shower counters, G: wire-spark chambers.

$$\frac{d^3\sigma}{dp^3} = A + \epsilon C + \epsilon B \cos 2\phi + [\epsilon(\epsilon + 1)/2]^{1/2} D \cos \phi. \quad (4)$$

The results presented here have been averaged over  $\phi$  so as to eliminate the  $B$  and  $D$  terms.

The data are presented in terms of the invariant-structure function  $F(x', Q^2, W)$  obtained by averaging

$$\frac{E}{\sigma_T} \frac{d^3\sigma}{dp^3} = \frac{E^*}{\sigma_T} \frac{2}{(p_{\max}^{*2} - p_T^2)^{1/2}} \frac{d^3\sigma}{dx' dp_T^2 d\phi} \quad (5)$$

over the range  $p_T^2 < 0.02 \text{ GeV}^2$  and  $0 < \phi < 2\pi$ . Here  $\sigma_T$  is the total virtual-photon-nucleon cross sec-

tion. The proton total cross section,  $\sigma_p$ , was taken from a fit to the SLAC-MIT results with  $\sigma_s/\sigma_t = 0.18$ .<sup>8</sup> The deuteron total cross section,  $\sigma_d$ , was calculated from the expression  $\sigma_d = \sigma_p(2 - 0.75/\omega)$ .<sup>9</sup>

### III. APPARATUS AND DATA REDUCTION PROCEDURE

The two-arm spectrometer system shown in Fig. 1 was used to obtain data with a hydrogen target at the  $(W, Q^2)$  points  $(2.2 \text{ GeV}, 1.2 \text{ GeV}^2)$ ,  $(2.7, 2.0)$ ,  $(2.7, 3.3)$ ,  $(2.7, 6.2)$ , and  $(2.7, 9.5)$  and with a deuterium target at  $(2.2, 1.2)$ ,  $(2.7, 2.0)$ ,  $(2.7, 6.2)$ , and  $(2.7, 9.5)$ . A lead-Lucite shower counter was used to identify the scattered elec-

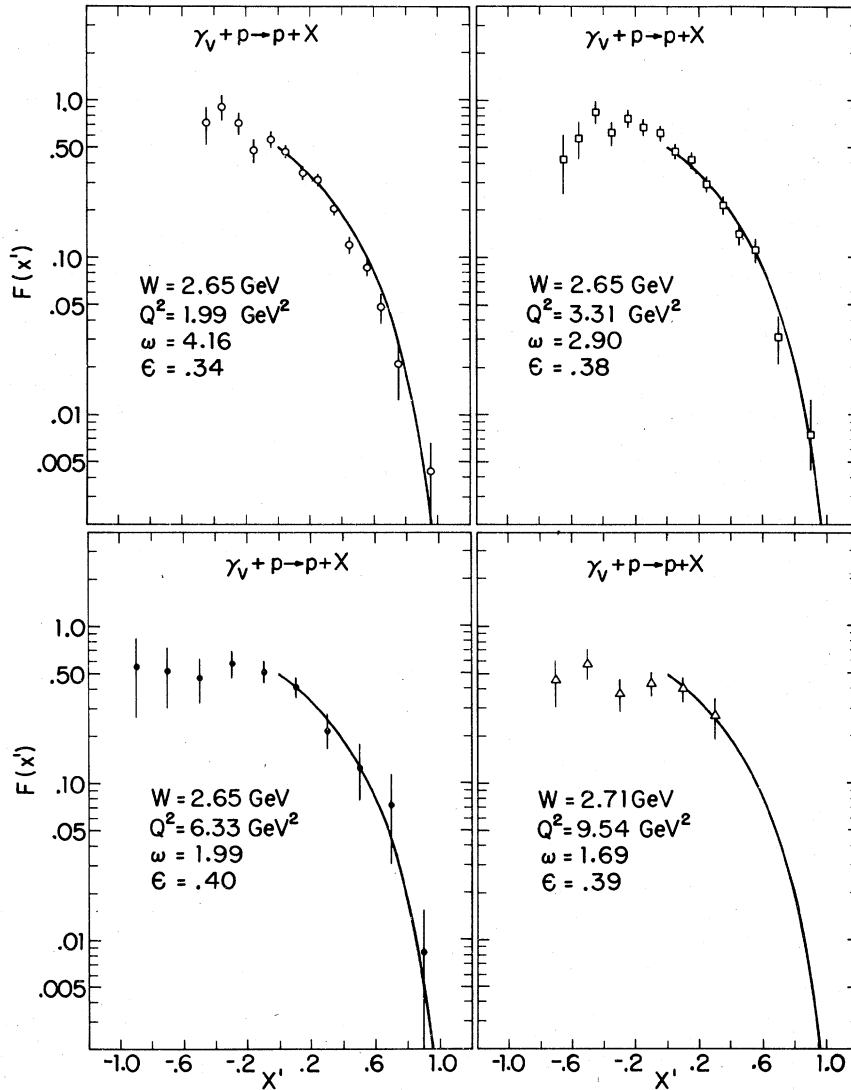


FIG. 2. The proton structure function for a proton target at  $W \approx 2.7 \text{ GeV}$  for several values of  $Q^2$  and  $p_T^2 < 0.02 \text{ GeV}^2$ . The solid line is the same in all four figures. It is given by  $0.49(1 - x')^2$  and is the best fit to all four data points over the region  $0 < x' < 1$ .

trons. Pions were eliminated by their time of flight for momenta less than 1.8 GeV and by a threshold Freon Čerenkov counter for momenta greater than 1.8 GeV. The data have been corrected for random coincidences ( $\sim 2\%$ ), electronics dead time ( $\sim 5\%$ ), absorption in the counters ( $\sim 6\%$ ), and target-wall events ( $\sim 2\%$ ). The correction for pion background on the electron arm ranged from 5 to 30%, with an estimated error equal to 10% of the correction. The uncertainties shown in the figures are statistical only and do not include the overall systematic error which is estimated to be less than  $\pm 8\%$ . An estimate has been made of the electron radiative correction. It varies from 0 to 50% as  $x'$  varies from 0 to 1 and, at fixed  $x'$ , varies only about 5% among the  $(W, Q^2)$  points. No radiative corrections have been applied to the data.

#### IV. RESULTS

Figures 2 and 3 show the proton structure function for a proton target as a function of  $x'$  for  $p_T^2 < 0.02 \text{ GeV}^2$ . The solid line in Figs. 2 and 3 is

$$F(x') = 0.49(1 - x')^n \quad (6)$$

with  $n=2$ . This line is the best fit to the four data points shown in Fig. 2 for  $0 < x' < 1$  with  $n$  constrained to equal 2; the error in the coefficient is 0.01. Theory<sup>1</sup> predicts that for  $x' \sim 1$  the invariant structure function will have the form of Eq. (6) with  $n = 1 - 2\alpha$ . Here  $\alpha$  is the Regge parameter which

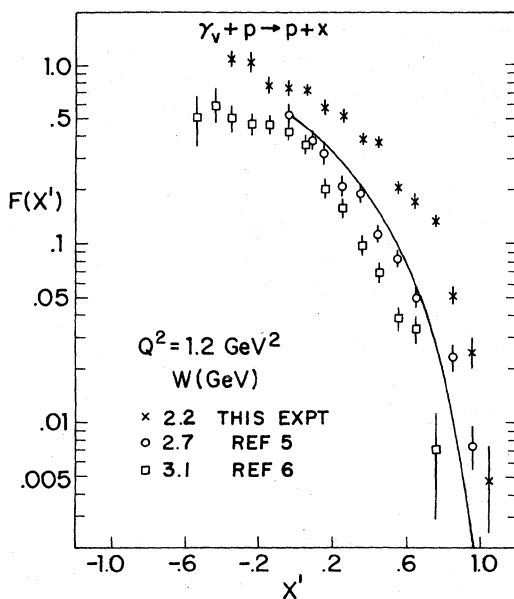
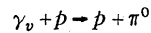


FIG. 3. The proton structure function at fixed  $Q^2 = 1.2 \text{ GeV}^2$  and several values of  $W$ . For these data  $p_T^2 < 0.02 \text{ GeV}^2$ . The solid curve is the same as that shown in Fig. 1.

characterizes the energy dependence of the exclusive reaction to which the inclusive reaction is linked in the correspondence principle limit. For simple nucleon exchange corresponding to the reaction



$\alpha(0) \sim -0.5$  and  $n=2$ .

The figures show that for  $W = 2.67 \text{ GeV}$  Eq. (6) describes the shape of the invariant structure function quite well over the surprisingly large  $x'$  range,  $x' > 0$ . Figure 2 also shows that the invariant structure function is independent of  $Q^2$  at fixed  $W$ . This independence of  $Q^2$  is the dominant feature of the inclusive electroproduction reactions. Figure 3 shows that at fixed  $Q^2$  the invariant structure function changes with  $W$ . The  $(2.15\text{-GeV}, 1.2\text{-GeV}^2)$  and  $(2.65, 1.99)$  data displayed in Figs. 3 and 2, respectively, have the same value of  $\omega$ ,  $\omega = 4.16$ . They differ substantially and show that the invariant structure function for forward protons does not display Bjorken scaling.

Figure 4 shows the ratio of the invariant structure function for protons from a deuterium target to that for protons from a proton target at  $W = 2.7 \text{ GeV}$ . These data suggest that the invariant structure function for forward protons from a neutron

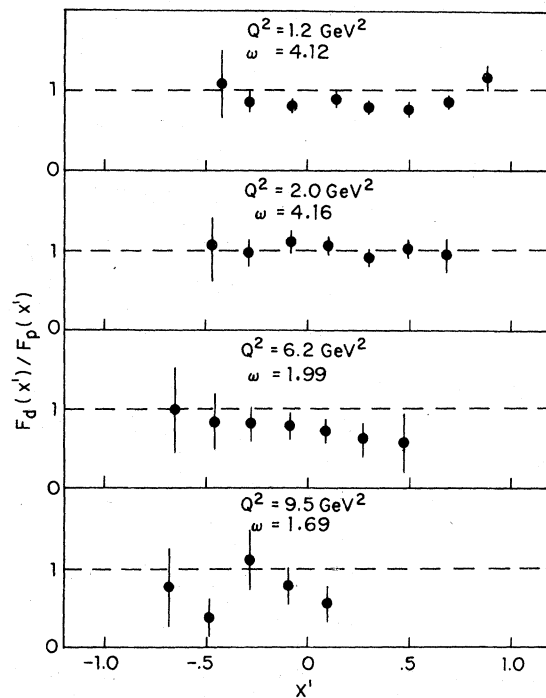


FIG. 4. The ratio of the invariant structure function for protons from a deuterium target to that for protons from a proton target as a function of  $Q^2$  at  $W \approx 2.7 \text{ GeV}$ . For these data  $p_T^2 < 0.02 \text{ GeV}^2$ .

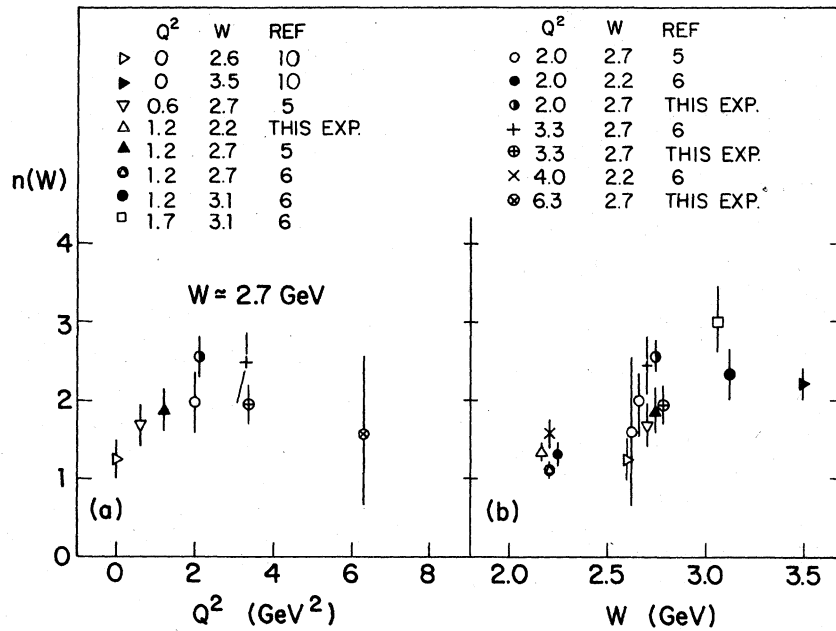


FIG. 5. Results for the values of the parameter  $n$  for a fit to the proton structure function of the form  $A(1-x')^n$  in the region  $0.2 < x' < 1.0$ . Part (a) shows the value of  $n$  versus  $Q^2$  for the data with  $W \approx 2.7$  GeV. Part (b) shows the value of  $n$  versus  $W$ , the total energy in the virtual-photon-target-proton center-of-mass system.

target is somewhat less than from a proton target.

In order to study the behavior of the data more closely, the structure functions for the proton target have been fit to the form

$$F(x') = A(1-x')^n \tag{7}$$

for  $x' > 0.2$ . Figure 5 shows the values of  $n$  as a function of  $W$  for the data of this experiment and

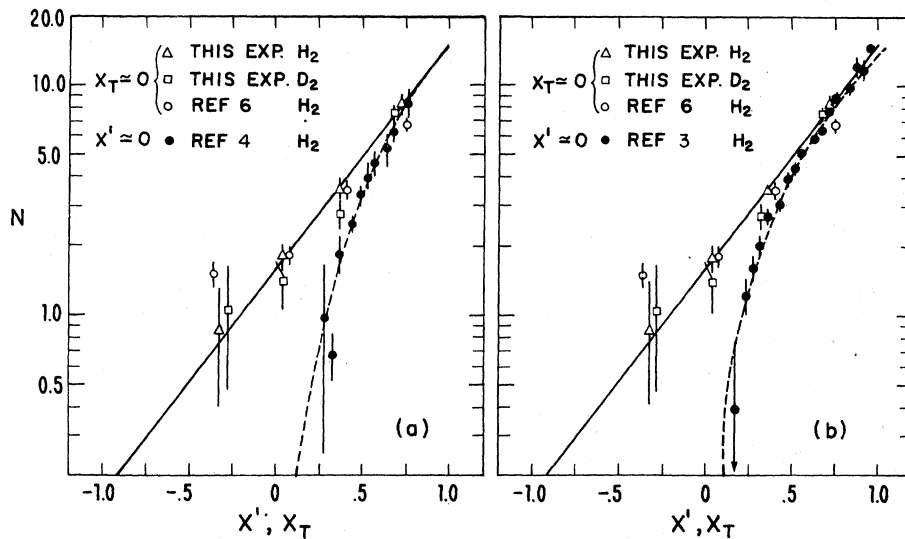


FIG. 6. (a) The parameter  $N$ , plotted versus  $x'$  or  $x_T$ , obtained from a fit to the proton structure function of the form  $f(x')/W^N$  for forward protons and  $f(x_T)/W^N$  for protons produced between  $100^\circ$  and  $150^\circ$  in the virtual-photon-target-proton center-of-mass system. The solid curve is a fit to the forward-proton data; the dashed curve is a fit to the large-angle data. (b) The parameter  $N$ , plotted versus  $x'$  or  $x_T$ , obtained from a fit to the proton structure function of the form  $f(x')/W^N$  for forward protons and  $f(x_T)/W^N$  for pions produced near  $90^\circ$  in the virtual-photon-target-proton center-of-mass system. The solid curve is a fit to the forward-proton data; the dashed curve is a fit to the pion data.

other reported measurements of inclusive proton electroproduction<sup>5,6</sup> and photoproduction.<sup>10</sup> At  $W = 2.7$  GeV, where there is the most data, the electroproduction data indicate that for fixed  $W$  there is no dependence on  $Q^2$  and at  $W = 3.1$  GeV it exceeds the value  $n = 2$  predicted by the simple form of the Regge theory.

Another parameterization of the data which is suggested by measurements of proton electroproduction between  $100^\circ$  and  $150^\circ$  in the virtual-photon-target-nucleon center-of-mass system<sup>4</sup> is

$$F(x') = f(x')/W^N, \quad (8)$$

where  $N$  is a function of  $x'$ . Figure 6 shows a plot of the fit value of  $N$  versus  $x'$  for the new data reported here and the data from an earlier experiment<sup>6</sup> together with the values determined from a similar fit to measurements of protons produced between  $100^\circ$  and  $150^\circ$  in the virtual-photon-target-proton center-of-mass system.<sup>4</sup> A fit to the new hydrogen data reported here gives

$$N(x') = (1.57 \pm 0.10) \exp[(2.26 \pm 0.13)x'], \quad (9)$$

where the  $\chi^2/\text{DOF}$  is 0.2/2. This is shown as a solid curve in Figs. 6(a) and 6(b). Figure 6(b) shows the fit values of  $N$  versus  $x'$  for the forward-proton data together with the values of  $N$  determined from a similar fit to measurements of pions produced at  $90^\circ$  in the virtual-photon-target-proton center-of-mass system.<sup>3</sup>

Near  $x' \approx 1$  the energy dependence for forward protons is the same as that for sidewise protons

and pions where  $x_T = p_T/p_{\text{max}}^* \approx 1$ . This behavior can be understood in terms of the correspondence principle<sup>11</sup> and it suggests that, in the framework of the constituent-interchange model,<sup>12,13</sup> the energy dependence is determined by the quark reactions allowed by the exchange or interchange of quark fields using the elementary two-field and three-field hadron wave functions which are linked to the  $\gamma_v p \rightarrow p\pi^0$  and  $\gamma_v p \rightarrow p\pi^+\pi^-$  exclusive channels.

## V. CONCLUSIONS

In conclusion the proton structure function is independent of  $Q^2$  at fixed  $W$  but shows a strong dependence on  $W$  at fixed  $Q^2$ . For  $x' > 0.2$  the invariant structure function can be described by the expression  $(1 - x')^n$ , where  $n$  is a function of  $W$  which for  $W \approx 2.7$  GeV is not inconsistent with the value  $n = 2$  predicted by the Regge model through the inclusive-exclusive connection. The observed  $W$  dependence at  $x' \approx 1$  is very similar to that observed for inclusive electroproduction of protons and pions at high transverse momenta and suggests that both kinematic regions have a similar explanation in terms of the constituent-interchange model.

## VI. ACKNOWLEDGMENTS

We wish to acknowledge the support of Professor Boyce McDaniel, the staff of the Wilson Synchrotron Laboratory, and the staff of the Harvard High Energy Physics Laboratory.

\*Research supported in part by Energy Research and Development Administration (Harvard) and National Science Foundation (Cornell).

†Present address: Fermi National Accelerator Laboratory, P. O. Box 500, Batavia, IL. 60510.

‡Present address: 36 Webb St., Lexington, MA. 02173.

§Present address: Clinton P. Anderson Laboratory, Los Alamos, NM. 87545.

<sup>1</sup>R. P. Feynman, *Photon-Hadron Interactions* (Benjamin, Reading, Mass., 1972).

<sup>2</sup>C. J. Bebek *et al.*, *Phys. Rev. Lett.* **37**, 1525 (1976).

<sup>3</sup>A. Browman *et al.*, *Phys. Rev. Lett.* **37**, 651 (1976).

<sup>4</sup>A. Browman *et al.*, *Phys. Rev. Lett.* **37**, 974 (1976).

<sup>5</sup>C. J. Bebek *et al.*, *Phys. Rev. Lett.* **32**, 27 (1974).

<sup>6</sup>C. J. Bebek *et al.*, *Phys. Rev. Lett.* **34**, 1115 (1975).

<sup>7</sup>L. Hand, *Phys. Rev.* **129**, 1834 (1963).

<sup>8</sup>W. B. Atwood, private communication.

<sup>9</sup>F. W. Brasse, in *Proceedings of the Sixth International Symposium on Electron and Photon Interactions, Bonn, Germany, 1973*, edited by H. Rollnik and W. Pfeil (North-Holland, Amsterdam, 1973), p. 251.

<sup>10</sup>H. Burfeindt *et al.*, *Phys. Lett.* **43B**, 345 (1973); *Nucl. Phys.* **B74**, 189 (1974).

<sup>11</sup>J. D. Bjorken and J. Kogut, *Phys. Rev. D* **8**, 1341 (1973).

<sup>12</sup>D. Sivers, S. J. Brodsky, and R. Blankenbecler, *Phys. Rep.* **23C**, 1 (1976).

<sup>13</sup>R. Blankenbecler and S. J. Brodsky, *Phys. Rev. D* **10**, 2973 (1974).